Available online at www.sciencedirect.com
SCIENCE DIRECT
Biochimica et Biophysica Acta 1758 (2006) 487–492
BIOCHIMICA ET BIOPHYSICA ACTA
BBA
http://www.elsevier.com/locate/bba

AFM study of interaction forces in supported planar DPPC bilayers in the presence of general anesthetic halothane

Z. Leonenko [a], E. Finot [b], D. Cramb [a,*]

[a] Department of Chemistry, University of Calgary, 2500 University Drive NW, Calgary, Canada AB T2N 1N4
[b] Laboratory of Physics, Nanosciences, University of Burgundy, 9 avenue A. Savary, BP 47870, F-21078 Dijon cedex, France

Received 15 November 2005; received in revised form 27 February 2006; accepted 28 February 2006
Available online 31 March 2006

Abstract

In spite of numerous investigations, the molecular mechanism of general anesthetics action is still not well understood. It has been shown that the anesthetic potency is related to the ability of an anesthetic to partition into the membrane. We have investigated changes in structure, dynamics and forces of interaction in supported dipalmitoylphosphatidylcholine (DPPC) bilayers in the presence of the general anesthetic halothane. In the present study, we measured the forces of interaction between the probe and the bilayer using an atomic force microscope. The changes in force curves as a function of anesthetic incorporation were analyzed. Force measurements were in good agreement with AFM imaging data, and provided valuable information on bilayer thickness, structural transitions, and halothane-induced changes in electrostatic and adhesive properties.

Keywords: Planar bilayer; Halothane; Microdomains; Force spectroscopy

1. Introduction

Changes in physical and chemical properties of biological membranes due to the partitioning of halothane is of great interest for understanding the mechanism of anesthetic action. The molecular theory of anesthetic action includes the hypothesis that the anesthetic alters the lipid membrane structure and therefore the biophysical properties of the membrane. Properties such as lateral pressure within bilayers [1], lipid packing in membranes [2–4], polarization of the membrane and the degree of motional disorder in lipid chains [16], which leads to the bilayer thinning [5–7], have all been associated with the partitioning of halothane into the bilayer. Atomic force microscopy (AFM) is a valuable technique to address the structural changes in the membrane. This technique has proven to be advantageous for imaging supported planar bilayers in liquid media [7–12].

AFM has also proven to be an advantageous tool for measurements of forces of interaction between the AFM probe and the surface, giving information about the physical properties of sample surface [13–15]. On approach of the AFM probe tip to the sample, repulsive forces can be measured, such as electrostatics, solvation, hydration, and compression-related steric forces. The retraction force curves often show a hysteresis referred to as an adhesion pull off event, which can be used to estimate the adhesion forces. Much experimental force data are now available in the literature, and theoretical models have been developed for the analysis of forces acting between two solid surfaces [16–20] and to a lesser extent the properties of thin films [21–25].

In a previous study, we demonstrated the existence of phase transitions in model membranes, such as DPPC (1,2-dipalmitoylphosphatidylcholine) mica-supported bilayers due to the partitioning of halothane and of ethanol into the bilayer [11]. We observed structural changes in the supported bilayer, such as changes bilayer area, and bilayer height (i.e., domain formation), which were dependent on time of incubation and concentration of anesthetics. Similar domain formation was observed when the membrane underwent a melting transition. In spite of the visual similarity of an anesthetic induced domain formation and the heat induced gel–liquid phase transition,

* Corresponding author: Fax: +1 403 289 9488.
E-mail address: dcramb@ucalgary.ca (D. Cramb).

0005-2736/$ - see front matter © 2006 Elsevier B.V. All rights reserved.
doi:10.1016/j.bbamem.2006.02.033

observed by AFM imaging, the mechanism of anesthetic action is likely to be different from the effect of membrane melting. In our earlier work [11] we performed analysis of interaction forces during a bilayer melting transition. Here, we extended force measurements and analysis to halothane-DPPC system in order to compare changes in bilayer physical properties due to two different processes: membrane melting and membrane interaction with anesthetic. To the best of our knowledge no force measurements were reported to date on halothane–lipid membrane system.

2. Materials and methods

1,2-Dipalmitoyl phosphatidylcholine (DPPC) (Avanti Polar-lipids Inc., Alabaster, ME) was used without further purification. Distilled, deionized, nanopure quality water was used in the generation of all vesicles. Freshly cleaved ASTMV-2 quality, scratch-free ruby mica (Asheville-Schoonmaker Mica Co., Newport News, VA) was used throughout this study as a substrate. All vesicles were prepared using the "dry" method as previously reported [8]. An appropriate aliquot of phospholipid chloroform solution was measured into a small vessel and the chloroform removed using a stream of dry nitrogen. The dry phospholipid was then resuspended in buffer to its final concentration and stirred for 30 min. The solution was sonicated (Branson 1200, Dansbury, CT) at room temperature for 10-min periods. Between each 10-min period, there was a 15-min "rest" interval where the solution was stirred at room temperature. For this method, the solutions were cycled an average of 10 times or until they were observed to clear.

Supported planar bilayers were prepared for AFM imaging by the method of vesicle fusion [8]. Aliquots of liposome solution were deposited on unmodified freshly cleaved mica. After a controlled period of time the mica was gently rinsed with nanopure water and the surface was imaged under water in the liquid cell at room temperature.

Halothane incorporation was performed by adding small volumes of pure anesthetic into the liquid cell, containing the established supported bilayer. The sample was incubated for 1.5 h and then the sample was rinsed with nanopure water. An incubation time of 1.5 h was shown by fluorescence experiments to be optimal for halothane partitioning between water and bilayer to reach equilibrium under similar conditions [26].

Surfaces were imaged with an atomic force microscope (Pico SPM, Molecular Imaging, Tempe, AZ) equipped with an AFMS-165 scanner. We employed MAC (magnetic A/C) mode AFM, where a magnetically-coated probe oscillates near its resonant frequency driven by an alternating magnetic field. The nominal spring constant of Au–Cr-coated Maclevers (Molecular Imaging) used was 0.6 N/m. The tip radius of curvature is quoted as being typically 25 nm. The scan rate was 20 μm/s. The standard MAC mode fluid cell (Molecular Imaging) was used throughout. All imaging and force measurements were performed in a liquid cell under nanopure water. The height scale was calibrated using colloidal gold spheres of well-defined size (diameter 5 and 14 nm) from commercial supplier Ted Pella Inc.

The atomic force microscope was also used as a force apparatus. The force spectroscopy experiment consists of monitoring the interaction between the AFM tip and the substrate by sensing the cantilever deflection, Z_c, as a function of the piezo elongation, Z_p, as the tip is moved toward and away from the substrate. Data were collected over a time period of 2 h and a total of 100 force curves was analyzed for each sample.

Force measurements were performed on DPPC bilayers formed from water solutions with and without halothane. It is a well-known fact that the forces of interactions depend on the velocity of the surface approach [16], especially for soft viscoelastic materials. All measurements were performed over five velocities: 0.5, 5, 50, 500 and 2500 nm/s. A maximum force of approximately 25 nN was maintained for all approach velocities. Thus, the different velocities provide different contact times with the surface. A statistical analysis has revealed that 10 measurements at different locations of the same area are required to determine parameters such as the adhesion and the long-range forces with ±10% accuracy. Force curves were monitored as a function of anesthetic incorporation at several different positions of the cantilever, chosen after the image was completed.

As the tip–sample separation cannot be independently measured, we developed a systematic procedure for calculating the sensitivity of the apparatus [11]. This measurement assumes that tip and the mica surface are brought into a nondeformable contact in the higher loading region. Raw data (Z_c versus Z_p) are then converted into force F versus surface-tip separation D using Hooke's law. $F=kZ_c$, where k is the spring constant of the cantilever, and the geometric relationship $D=Z_c-Z_p$ for incremental changes.

Statistical data were extracted from a large set of measurements. We used the Gaussian distribution in the following form:

$$P(x) = C\frac{1}{\sigma\sqrt{2\pi}}e^{-(x-\mu)^2/(2\sigma^2)} \quad (1)$$

where $P(x)$ is the number of samples at the particular point x in the histogram, μ the mean, σ the standard deviation, and C the normalization constant. The bin size of histogram is determined statistically by dividing the range of measurements by the square-root of the number of measurements. The average of the adhesion force and the standard deviation were obtained from the analysis of the whole set of the force curves which are represented in histogram form ($P(x)$) and then adjusted using a Gaussian law.

3. Results and discussion

A supported DPPC bilayer was formed on mica from vesicle solution, rinsed with water and covered with 1 ml of water in the AFM liquid cell. Pure halothane (60 μl) was added into the liquid cell and the cell was incubated for 1.5 h. After this, non-partitioned halothane was removed by gently rinsing and then refilling the cell with water. The bilayer was imaged in intermittent contact mode (MAC-mode) with a nominal force less than 1 nN. A typical image of the DPPC bilayer with halothane incorporated is shown in Fig. 1A. Halothane incorporation results in domain formation [7]. The surface coverage of the lower domains exceeded that of the higher domains for larger volumes of halothane added (up to 100 μL). The thickness of higher and lower domains was measured as 5.5 nm and 3.5 nm, respectively. The thickness of the pure DPPC bilayer is 5.5 nm. These results are consistent with our previous work [7,8], where comparisons to X-ray diffraction measurements were made. Moreover, we have examined and discussed previously the measurement of bilayer thickness using AFM [8]. We found that one must be very careful on the definition of thickness, that in AFM the measured thickness is sensitive to the forces used and that direct comparison between AFM and X-ray results are not always warranted.

Fig. 1B is the phase image of the halothane-treated bilayer, taken during the same scan as Fig. 1A. The contrast in phase images is often interpreted as differences in viscoelasticity or tip–surface energy dissipation [8]. The phase contrast between the higher and lower domains in Fig. 1 are quite striking and suggest a significant alteration in the tip–surface interactions between the domains. Thus, the domains differ not only in height, but possibly also in their surface structure and fluidity. It is possible that halothane is present in the higher domains as well as in lower domains, but to a lesser extent. Therefore non-uniform dark regions (in phase image) in an otherwise (topography image) uniformly higher domain might be the evidence of the presence of halothane and changes in electrostatic properties.

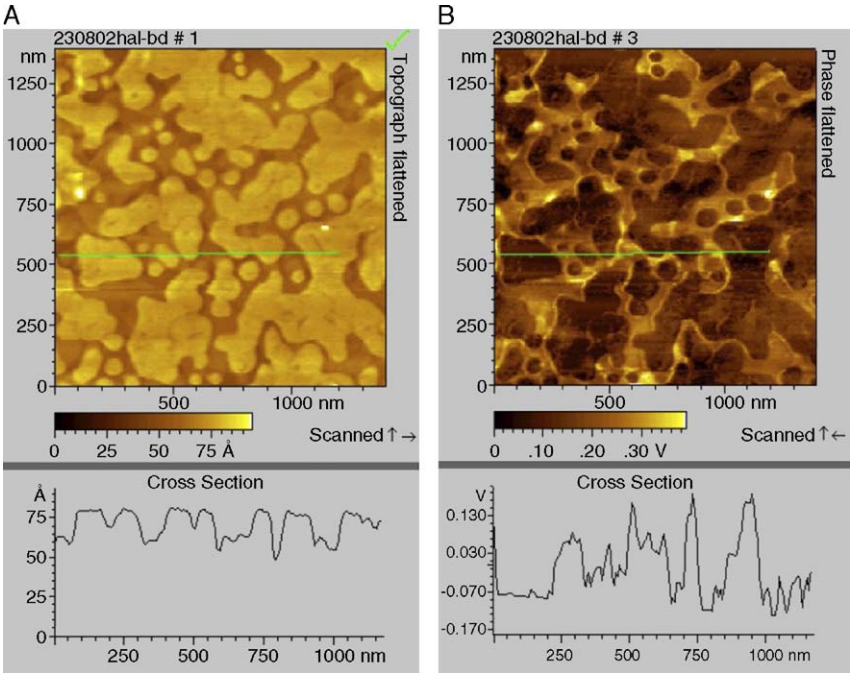

Fig. 1. (A) A typical topography AFM image of a DPPC bilayer with halothane incorporated. The supported bilayer was formed on mica from a vesicle solution, rinsed with water and covered with 1 ml of water in the AFM liquid cell. A volume of halothane (60 μl) was added into the liquid cell and the cell was incubated for 1.5 h. After this, non-partitioned halothane was removed by rinsing with water. The resulting bilayer was imaged in intermittent contact mode (Mac-mode). (B) The phase image taken during the same scan. The changes in phase represent changes in viscoelasticity of the bilayer.

The extent of domain formation observed here results from a mol ratio of halothane/lipid in the range 3–5 [7]. As discussed in our previous work [7,26], we acknowledge that concentration of halothane in the bulk solvent described here is much greater than the serum levels used in anesthesia. However, the concentration of anesthetic in neuronal membranes is not known and we [7] and others [27] have shown that incorporation of halothane into bilayers is likely a cooperative effect where halothane is distributed heterogeneously. Therefore, the local concentration of halothane within domains of the cell membrane may be quite high. Forces were measured in contact mode using the same image obtained in MAC mode. Force curves were collected at 10 locations on the lower domain of the bilayer and then averaged.

4. Forces between the DPPC bilayer and AFM tip as a function of halothane incorporation

4.1. Adhesion forces

Surface force profiles were measured between the silicon nitride tip and mica and a pure DPPC bilayer, or a DPPC bilayer with halothane partitioned into it. Raw data of the cantilever deflection corresponding to the retraction of the tip from the surface, after contact with the tip, are shown in Fig. 2A, plots a–d. The data corresponding to the mica surface immersed in water are presented for comparison. Mica was characterized by an abrupt jump out of contact, plot a.

The adhesion force acting on the DPPC bilayer, plot b, does not differ drastically from the mica substrate as might be expected for a gel phase bilayer (T_M=42 °C). Incorporation of halothane leads to a significant change of the force profile, plot d. The adhesion event originates from van der Waals' forces, which can be thought of in terms of the Hamaker constant. The Hamaker constant relates the tip–sample force to the tip–sample distance for a given geometry [28]. A bilayer adsorbed on mica is known to reduce the overall Hamaker constant [28]. Apparently, addition of halothane into the bilayer increases the Hamaker constant significantly as is indicated from the increased force at a given tip–sample distance (Fig. 2A), compared with that at large tip–sample distance. One most note also that there is an electrostatic component of the tip–sample

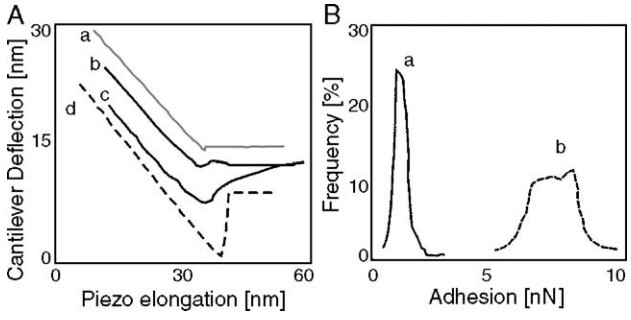

Fig. 2. (A) Cantilever deflection dZ_c as a function of the piezotube elongation when the tip is retracted from the sample. DPPC bilayers deposited on mica were measured under three conditions: (b) the DPPC bilayer at T=20 °C (c) the DPPC bilayer at T=50 °C (d) the DPPC bilayer with halothane incorporated. The adhesion curve on bare mica (a) is shown for comparison. (B) Distribution of adhesion force, measured on DPPC: Plot (a) DPPC at room temperature; Plot (b) DPPC with halothane.

Table 1
Experimental adhesion force F_{adh} and its standard error sigma on DPPC bilayer and DPPC with halothane, measured at room temperature; calculation of the number of bindings n and the mean force of a single bond F_s; (*) data on DPPC bilayer at room and elevated temperature, measured earlier during melting transition (11), are shown for comparison

	DPPC 22 °C	DPPC (*) 22 °C	DPPC+halothane 22 °C	DPPC (*) 60 °C
F_{adh}	1.5 nN	1 nN	7 nN	5 nN
σ	0.8 nN	0.6 nN	2 nN	2 nN
F_s	0.4 nN	0.3 nN	0.5 nN	0.8 nN
n	4	3	14	6

interaction. This will be discussed in the Repulsive Forces subsection.

This adhesion force behavior can be compared to that observed from our earlier work on the phase transition in DPPC from the gel to liquid crystal observed with increasing the temperature [11]. The temperature increase leads to a gradual increase of the adhesion force. The adhesion force acting on the DPPC at 50 °C is added in Fig. 2 A for comparison, plot c. As van der Waals forces are known to vary only slightly with temperature, we have previously attributed the increase in adhesion force to the phase transition that leads to an increase of the lipid tail mobility [11].The behavior of the adhesion forces, measured on the halothane-incorporated bilayer domains, is similar to what was observed with temperature induced phase transition. Therefore halothane induces the transition of bilayer into the fluid phase in a similar manner as melting. The statistical distribution of the adhesions forces, plotted in Fig. 2B, clearly demonstrates that adhesion forces observed for pure DPPC bilayer correspond to a sharper peak and a narrower distribution than that for DPPC with halothane. Incorporation of halothane leads to an increase in adhesion force.

To analyze adhesive forces we employed the same statistical analysis, as we used in our previous work [11]. It has been demonstrated that the force of a unit interaction between an AFM tip and a surface can be determined from a statistical analysis of a series of detachment force measurements. For a statistical analysis based on adhesive force originating from a discrete number n of individual interactions or bonds, F_s have been used. The total force distribution follows Poisson statistics, where both the adhesion force F_{adh} and the variance σ originates from a number of individual bonds n.

$$F_{adh} = nF_s \tag{2}$$

$$\sigma^2 = nF_s^2 \tag{3}$$

The force of one bond, F_s, is therefore given by the square of the variance of the force divided by the mean adhesion force F_{adh}. The value n is the ratio between F_{adh} and F_s. This analysis has the advantage that the knowledge of the mean radius of curvature is not required [29] and gives information on the nature of the bilayer. Table 1 presents the standard deviation of the adhesion force in the gel phase DPPC bilayer and bilayer with halothane incorporated, measured in this work. Data for gel phase DPPC bilayer at room temperature and fluid phase DPPC bilayer at elevated temperature from our previous paper [11] are shown for comparison.

The imaging characteristics of a fluid phase bilayer at high temperature are typically ascribed to a higher number of tip–sample bonds, as we have previously demonstrated [11]. The force of a single bond is increased in a fluid phase. The effect of halothane is similar to the effect of melting. DPPC bilayer with halothane corresponds to higher adhesion force, higher sigma, and larger amount of single binding events between the AFM tip and the sample. The number of tip–sample bonds, $n=14$, is more than two times larger when compared to 6 for fluid phase produced by melting. The single force F_s was not altered significantly by the presence of halothane. Therefore the presence of halothane in the bilayer increases the fluidity of the DPPC molecules in the bilayer. The number of binding events, n also could be higher due to the contribution of halothane molecules themselves, interacting with AFM tip. Additionally, we observed a dependence of the adhesion force on the scan rate (data not shown), which comes to reinforce the idea that phase transition from a liquid crystalline phase to the fluid phase is induced by halothane. F_{adh} for bilayer with halothane shows higher dependence on the scan rate, than the pure bilayer, this is a characteristic of the increased fluidity of the bilayer. An increase in mobility will increase the number of molecules in contact with the AFM probe, the larger n is, the higher F_{adh}.

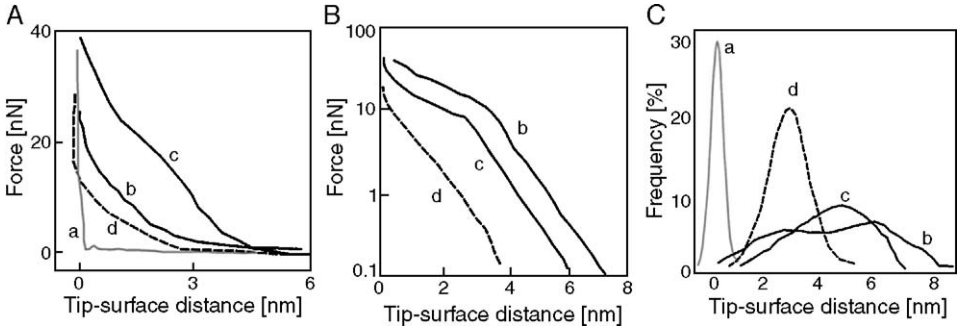

Fig. 3. (A) Surface force as a function of a tip–surface distance in liquid cell when the tip is approaching the sample; (B) logarithmic representation of data in panel (A); (C) distribution of the "effective thickness" determined from force analysis (A) on mica, DPPC and DPPC with halothane incorporated. Plots on A–C are ascribed as: (a) bare mica (is shown for comparison), (b) the DPPC layer at $T=22$ °C, (c) the DPPC layer at $T=50$ °C, (d) the DPPC layer with halothane, at $T=22$ °C.

4.2. Repulsive forces

Fig. 3A shows four patterns of the repulsive forces measured during the AFM tip approaching the sample surface of pure mica (plot a), DPPC bilayer at room temperature (plot b), DPPC bilayer at 50 C (plot c) [11], and DPPC bilayer with halothane (plot d). The zero force intercept from Fig. 3B was used to determine the "effective bilayer thickness" corresponding to the related tip–sample distance. For pure DPPC, at longer range above approximately 4 nm, the exponential regime clearly exists. The long range can be explained by electrostatic forces, due to the effective surface charge, which originates from water shielding. The short-range regime (between 0 and 4 nm) at the contact of the DPPC film is attributed to the deformation of film. We believe that the second regime corresponds to the steric force [7,8,11,24,25]. In the presence of halothane, Fig. 3B plot d, the long range electrostatic forces appear to be reduced, in the range above 4 nm. In this case, the force is mostly governed by the bilayer deformation, described by steric forces [16]. Therefore, it is clear that halothane changes the surface charge density of DPPC bilayer and suppresses the electrostatic forces by replacing water molecules and reducing water shielding of the lipid bilayer. This is consistent with the observations of Koubi et al. [27] who used molecular dynamics to examine the effect of halothane on a DPPC bilayer. They found that the magnitude for the electrostatic potential of the bilayer surface increased by a factor of 2 upon incorporation of halothane, where the mol fraction of halothane was 50% compared with lipid.

Moreover, in a steric force region of the tip–sample approach curve, lower forces are required to compress the bilayer containing halothane. This could be due to a less "free" space in a halothane incorporated bilayer allocated to the lipid headgroups, because the halothane molecules take up room that the headgroups would have occupied, which correlates with the increased order in the lipid head groups observed by molecular dynamics simulations [27]. This might lead to the increased disorder in the lipid tails organization, and affect the binding and apparent fluidity of the bilayer compared with a liquid phase bilayer induced by heating.

Histograms of the effective thicknesses are shown in Fig. 3C. These distributions were generated from 5 force measurements at various positions on the bilayer surface and represent distributions about an mean measured force. The distribution of the effective thickness is relatively broad for DPPC at room temperature, Fig. 3C plot b, and two broad peaks are overlapped, one has maximum at 6 nm and the other one around 3 nm. We previously suggested that this results from two force regimes [11], as the tip approaches the bilayer. At longer distances, electrostatic interactions dominate the tip–bilayer interactions. At shorter distances, the tip is compressing the bilayer more severely and therefore steric crowding of the tails dominates. For DPPC with halothane, plot d, only one regime is observed. Only one well-defined peak centered at approximately 3 nm is observed in the histogram of the effective thickness. In the presence of halothane, the effective thickness of 3 nm tends to decrease by 1 nm compared to pure DPPC in the liquid phase. It is interesting to compare the force analysis and the height measured by image cross-section. The image cross-sections give 3.5 nm (Fig. 1, and [7] which is slightly more than the mean value shown in Fig. 3C but corresponds to the upper limit of the distribution.

Our findings correlate well with recently published results of molecular dynamics simulations [27,30] which reported the increase of area per lipid with the increase of halothane concentration. The increase in area per lipid would be a good reason to observe the increased fluidity and higher adhesion forces, which indeed is the case in our experiments.

5. Conclusions

The temperature induced phase transition of the DPPC has been already characterized by a decrease in the "effective thickness". Here we observed similar behavior for bilayers containing halothane. The major difference comes from the fact that the incorporation of halothane changes the electrostatic interaction which was not the case during the melting transition. Halothane is a small polar molecule and is assumed to increase the polarity of the bilayer at the interface, and has been shown to replace water molecules bound to lipids at the interface. Our force measurements confirmed that assumption and clearly showed the differences in bilayer physical properties in thin domains, produced by the melting transition and partitioning of halothane, but that the processes of melting and halothane-induced bilayer thinning are not exactly the same.

Acknowledgements

Financial support from NSERC (DTC) is gratefully acknowledged.

References

[1] R.S. Cantor, Breaking the Meyer–Overton rule: predicted effects of varying stiffness and interfacial activity on the intrinsic potency of anesthetics, Biophys. J. 80 (2001) 2284–2297.
[2] E.S. Rowe, Induction of lateral phase separations in binary lipid mixtures by alcohol, Biochemistry 26 (1987) 46–51.
[3] S.A. Simon, T.J. McIntosh, Interdigitated hydrocarbon chain packing causes the biphasic transition behavior in lipid alcohol suspensions, Biochim. Biophys. Acta 773 (1984) 169–172.
[4] P. Nambi, E.S. Rowe, T.J. McIntosh, Studies of the ethanol-induced interdigitated gel phase in phosphatidylcholines using the fluorophore 1,6-diphenyl-1,3,5-hexatriene, Biochemistry 27 (1988) 9175–9182.
[5] J. Mou, J. Yang, C. Huang, Z. Shao, Alcohol induces interdigitated domains in unilamellar phosphatidylcholine bilayers, Biochemistry 33 (1994) 9981–9985.
[6] R.L. McClain, J.J. Breen, The image-based observation of the L beta I-to-L-beta' phase transition in solid-supported lipid bilayers, Langmuir 17 (2001) 5121–5124.
[7] Z. Leonenko, D. Cramb, Thinned bilayer domain formation caused by incorporation of volatile anesthetics into supported phospholipid bilayers, Can. J. Chem. 82 (2004) 1128–1138.
[8] Z.V. Leonenko, A. Carnini, D.T. Cramb, Supported planar bilayer formation by vesicle fusion: the interaction of phospholipid vesicles with surfaces and the effect of gramicidin on bilayer properties using atomic force microscopy, Biochim. Biophys. Acta 1509 (2000) 131–147.
[9] W. Han, S.M. Lindsay, T. Jing, Magnetically driven oscillating probe microscope for operation in liquids, Appl. Phys. Lett. 69 (1996) 1–3.

[10] W. Han, S.M. Lindsay, Probing molecular ordering at a liquid–solid interface with a magnetically oscillated atomic force microscope, Appl. Phys. Lett. 72 (1998) 1656–1658.
[11] Z.V. Leonenko, E. Finot, H. Ma, T. Dahms, D.T. Cramb, Investigation of temperature induced phase transitions in DOPC and DPPC phospholipid bilayers using temperature-controlled scanning force microscopy, Biophys. J. 86 (2004) 3783–3793.
[12] P.E. Milhiet, V. Vie, M.C. Gioconde, C. Le Grimellec, AFM characterization of model rafts in supported bilayers, Single Mol. 2 (2001) 109–112.
[13] H.H.P. Fang, K.-Y. Chan, L.-C. Xu, Quantification of bacterial adhesion forces using atomic force microscopy (AFM), J. Microbiol. Methods 40 (2000) 89–97.
[14] B. Beech, J.R. Smith, A.A. Steele, I. Penegar, S.A. Campbell, The use of atomic force microscopy for studying interactions of bacterial biofilms with surfaces, Colloids Surf. B: Biointerfaces 23 (2002) 231–247.
[15] A.J. Engler, L. Richert, J.Y. Wong, C. Picart, D.E. Discher, Surface probe measurements of the elasticity of sectioned tissue, thin gels and polyelectrolyte multilayer films: correlations between substrate stiffness and cell adhesion, Surf. Sci. 570 (2004) 142–154.
[16] B. Cappella, G. Dietler, . Force-distance curves by atomic force microscopy, Surf. Sci. Rep. 34 (1999) 1–104.
[17] T.J. Senden, C.J. Drummond, P. Kékicheff, Atomic force microscopy: imaging with electrical double layer interactions, Langmuir 10 (1994) 358–362.
[18] J.P. Cleveland, E. Schäffer, K. Hansma, Probing oscillatory hydration potentials using thermal–mechanical noise in an atomic-force microscope, Phys. Rev., B 52 (1995) 8692–8695.
[19] S. Biggs, Steric and bridging forces between surfaces bearing adsorbed polymer: an atomic force microscopy study, Langmuir 11 (1995) 156–162.
[20] Y.F. Dufrêne, T. Boland, J.W. Schneider, W.R. Barger, G.U. Lee, Characterization of the physical properties of model biomembranes at the nanometer scale with the atomic force microscope, Faraday Discuss. 111 (1998) 79–94.
[21] E.W. van der Vegte, G. Hadziioannou, Scanning force microscopy with chemical specificity: an extensive study of chemically specific tip–surface interactions and the chemical imaging of surface functional groups, Langmuir 13 (1997) 4357–4368.
[22] E.K. Dimitriadis, F. Horkay, J. Maresca, B. Kachar, R.S. Chadwick, Determination of elastic moduli of thin layers of soft material using the atomic force microscope, Biophys. J. 82 (2002) 2798–2810.
[23] V. Franz, S. Loi, H. Muller, E. Bamberg, H.-J. Butt, Tip penetration through lipid bilayers in atomic force microscopy, Colloids Surf., B 23 (2002) 191–200.
[24] H.J. Butt, V. Franz, Rupture of molecular thin films observed in atomic force microscopy. I. Theory, Phys. Rev., E 66 (2002) 031601.
[25] S. Loi, G. Sun, V. Franz, H.J. Butt, Rupture of molecular thin films observed in atomic force microscopy. II. Experiment, Phys. Rev., E 66 (2002) 1602.
[26] A. Carnini, H.A. Phillips, L.G. Shamrakov, D.T. Cramb, Revisiting lipid—General anesthetic interactions: II. Halothane location and changes in lipid bilayer microenvironment monitored by fluorescence, Can. J. Chem. 82 (2004) 1139–1149.
[27] L. Koubi, M. Tarek, M.L. Klein, D. Scharf, Distribution of halothane in a dipalmitoyl phosphatidylcholine bilayer from molecular dynamics calculations, Biophys. J. 78 (2000) 800–811.
[28] J.N. Israelachvili, Intermolecular and Surface Forces, Academic Press, New York, 1992.
[29] J.M. Williams, T. Han, T.P. Beebe Jr., Determination of single bond forces from contact force variances in atomic force microscopy, Langmuir 12 (1996) 1291–1295.
[30] M. Pickholz, L. Saiz, M.L. Klein, Concentration effects of volatile anesthetics on the properties of model membranes: a coarse-grain approach, Biophys. J. 88 (2005) 1524–1534.